URSI GASS 2026, Kraków, Poland, 15 – 22 August 2026

Impact of Access-Point Placement on Path Loss and Temporal Dispersion in an Indoor Corridor at 28 and 38 GHz

Tomasz Grasza[(1)], Jarosław Wojtuń[(1)], Cezary Ziółkowski[(1)], Jan M. Kelner[(1)], and Aniruddha Chandra[(2)]
(1) Institute of Communications Systems, Military University of Technology, Warsaw, Poland
(2) ECE Department, National Institute of Technology, Durgapur 713209, WB, India

Abstract

A comprehensive indoor measurement campaign was carried out in a line-of-sight corridor environment at carrier frequencies of 28 GHz and 38 GHz using a wideband FMCW channel sounding system with 900 MHz bandwidth. Measurements were performed along the same propagation path for two representative access point placement scenarios, corresponding to a transmitter located on the corridor centerline and in the corridor corner. The receiver was moved along the corridor over distances from 5 m to 60 m with a 5 m step. The analysis of the measured channel impulse responses reveals noticeable differences between the two transmitter locations in terms of temporal dispersion characteristics. For both frequency bands, the corner-mounted transmitter generally leads to increased RMS delay spread at short and medium distances, with observed values exceeding those of the centerline configuration by up to several hundred nanoseconds at selected locations. Similarly, the mean delay exhibits stronger fluctuations for the corner–center scenario, indicating a higher contribution of reflected and diffracted propagation paths. The obtained results demonstrate that the transmitter location has a pronounced impact on both large-scale path loss and time-domain dispersion metrics, including mean delay and RMS delay spread. These observations highlight the critical role of access point placement in shaping propagation conditions in indoor mmWave corridors and provide valuable insights for the design and deployment of high-frequency wireless networks.

1. Introduction

Millimeter-wave (mmWave) frequency bands play a crucial role in contemporary and future wireless communication systems, including fifth generation (5G) networks and beyond, due to the availability of large contiguous bandwidths and the potential to achieve very high data rates [1]. At the same time, radio-wave propagation at mmWave frequencies is strongly influenced by environmental characteristics, antenna placement, and blockage effects, which necessitates accurate channel characterization.

Indoor environments constitute a particularly important and challenging application area for mmWave systems. Corridors are among the most common locations for wireless access-point deployment in office buildings, university facilities, and public infrastructures. Owing to their elongated geometry, corridors often provide line of-sight (LOS) propagation over relatively long distances, while simultaneously exhibiting pronounced waveguiding effects, multiple reflections from walls, floor, and ceiling, and high sensitivity to antenna positioning [2] – [4].

Previous indoor measurement campaigns have primarily focused on path-loss modeling and general channel statistics, often assuming a centrally located transmitting antenna [1]. In practical deployments, however, access points are frequently installed near corridor walls or corners due to architectural constraints, power-supply availability, or installation requirements. Such variations in access-point placement can significantly affect both large-scale propagation characteristics, such as signal attenuation, and temporal channel properties, including the structure of the PDP.

Despite its practical relevance, the impact of access-point placement in indoor corridors, particularly the comparison between centerline and corner installations, has not yet been sufficiently investigated at mmWave frequencies. Furthermore, comparative studies covering multiple carrier frequencies under identical propagation conditions remain limited.

This paper presents a comprehensive indoor corridor channel measurement campaign conducted at carrier frequencies of 28 GHz and 38 GHz under LOS conditions. Measurements were performed along the same measurement route and for identical transmitter receiver separation distances, considering two representative access-point configurations: a transmitting antenna positioned along the corridor centerline (Fig. 1, A) and a transmitting antenna placed near the corridor corner (Fig. 1, B). The transmitting antenna represents a mmWave access point and is equipped with a directional horn antenna, while the receiving antenna depending on the measurement scenario exhibits either directional or omnidirectional radiation characteristics and is moved along the corridor with a fixed spatial step.

The main contributions of this work are summarized as follows:

- an extensive wideband measurement campaign based on a 900 MHz FMCW waveform conducted at 28 GHz and 38 GHz in an indoor corridor under LOS conditions,
- extraction of path-loss characteristics and temporal dispersion parameters derived from measured PDP as functions of distance,
- A comparative analysis of the impact of access-point placement (corridor centerline versus corner) on indoor mmWave channel properties, leading to practical conclusions relevant to indoor network planning.

The results obtained confirm that access-point placement has a significant influence on both signal attenuation and temporal dispersion in indoor corridor channels, with the observed effects being strongly frequency dependent.

2. Measurement Scenario and Testbed

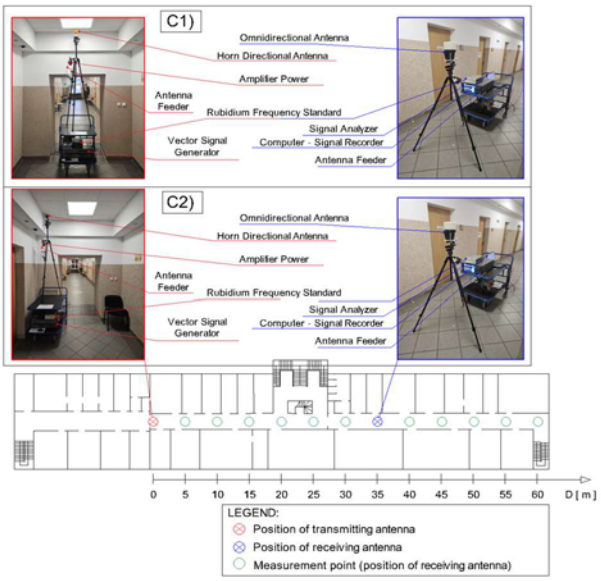


Fig. 1. Corridor measurement setup and layout used in the 28 GHz and 38 GHz campaigns: C1) first measurement configuration, C2) second measurement configuration. The figure illustrates the transmitter and receiver configurations, instrumentation, fixed transmitter position, and movable receiver measurement points along the Tx–Rx distance D.

Indoor channel measurements were conducted in a building corridor at carrier frequencies of 28 GHz and 38 GHz using an FMCW-based channel sounding system. Two propagation scenarios were considered: center–center and corner–center. The transmitting antenna (Tx), equipped with a directional horn antenna, was mounted near the ceiling at a fixed location, while the receiving antenna (Rx) with an omnidirectional radiation pattern was positioned at a height of 1.5 m and moved along the corridor in 5 m increments over a total distance of 60 m. A 900 MHz bandwidth FMCW waveform was transmitted, and complex IQ samples were recorded at a sampling frequency of 1.2 GHz. For each measurement configuration, carrier frequency, and Tx–Rx separation, the reference impulse was compared with impulses averaged from 999 recorded waveforms acquired by the signal analyzer. The averaging process was applied to reduce the impact of measurement noise and residual signal variations, thereby improving the robustness and repeatability of the extracted path loss and temporal dispersion metrics.

3. Channel Metrics and Definitions

The characterization of the indoor millimeter-wave radio channel was performed using well-established large-scale and time-domain metrics commonly applied in wideband propagation studies [1] – [4]. The analysis was based on the PDP, derived from the recorded complex-valued samples of the received signal, which describes the distribution of the received signal energy in the delay domain.

This metric represents the large-scale attenuation characteristics of the channel and enables a quantitative comparison of different access point placement scenarios in corridor environments (Fig. 1).

The time dispersion properties of the channel were described using the mean delay and the root mean square (RMS) delay spread, both derived from the normalized power delay profile.

The mean delay is defined as the first moment of the PDP and represents the center of gravity of the received signal energy in the delay domain:

$$\bar{\tau} = \frac{\sum_i \tau_i P(\tau_i)}{\sum_i P(\tau_i)} \quad (1)$$

The RMS delay spread is defined as the square root of the second central moment of the PDP:

$$\sigma_\tau = \sqrt{\frac{\sum_i (\tau_i - \bar{\tau})^2 P(\tau_i)}{\sum_i P(\tau_i)}} \quad (2)$$

The RMS delay spread quantifies the temporal dispersion of multipath components around the mean delay and is directly related to the frequency selectivity of wideband communication systems [2], [4].

The adopted metrics are widely used in indoor channel analysis and allow for a consistent assessment of the influence of corridor geometry and access point placement on millimeter-wave propagation, as illustrated by the measurement configurations in Fig. 1 and the results presented in Fig. 3–Fig. 6.

4. Results and Discussion

This section presents and discusses the results of radio channel measurements. The analysis begins with the RMS

delay spread and is subsequently followed by an evaluation of signal propagation losses expressed as path loss.

4.1 RMS delay spread

Figure 2 illustrates the method used to determine the tilt angle α of the transmitting antenna based on the geometry of the measurement setup. The method considers the difference in antenna heights as well as the distance between the TX and the RX.

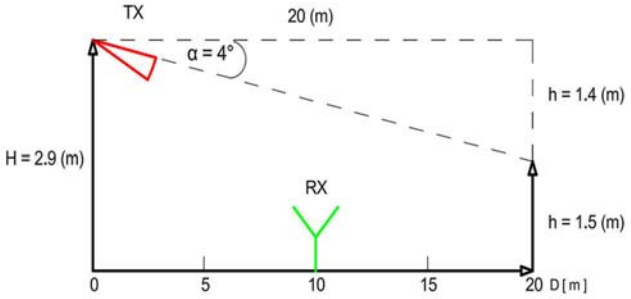


Fig. 2. Method for determining the tilt angle α of the transmitting antenna based on the geometry of the measurement setup.

Table 1 presents the RMS delay spread statistics obtained for the measurement scenarios at 28 GHz and 38 GHz. Scenario C1 corresponds to a center–center Tx–Rx antenna configuration, whereas scenario C2 represents a corner–center configuration, in which the transmitter is located at the corner and the receiver is positioned at the center of the measurement area.

Table. 1. RMS delay spread statistics for the measurement scenarios at 28 GHz and 38 GHz.

	28 GHz		**38 GHz**	
	C1 (ns)	**C2 (ns)**	**C1 (ns)**	**C2 (ns)**
Mean	69.54	73.93	179.52	168.59
Median	66.58	69.86	144.44	147.11
Standard Deviation	16.79	22.73	132.00	91.42

Based on the data presented in Table 1, it can be observed that scenario C1 generally exhibits lower RMS delay spread values compared to scenario C2 at 28 GHz, while the opposite trend is observed for the 38 GHz band.

The reduced delay spread in scenario C1 at 28 GHz and in scenario C2 at 38 GHz indicates lower temporal dispersion caused by multipath propagation, which improves signal time consistency and enhances transmission stability. Consequently, the preferred measurement configuration depends on the operating frequency, with scenario C1 being more favorable at 28 GHz and scenario C2 providing more advantageous propagation conditions at 38 GHz.

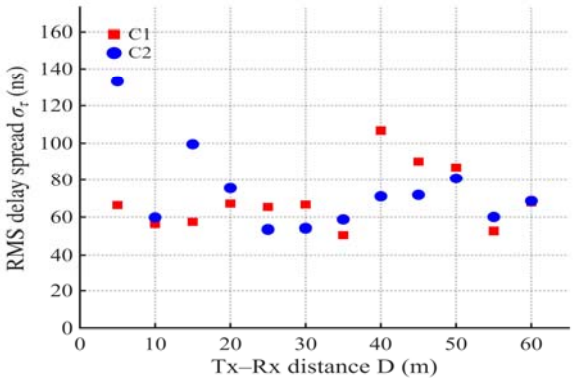


Fig. 3. RMS delay spread versus Tx–Rx distance at 28 GHz for LOS propagation, comparing antenna configurations C1 and C2.

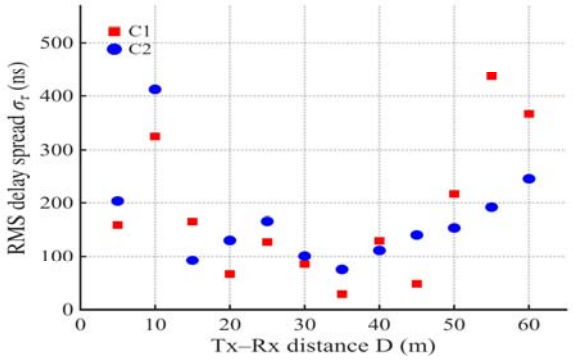


Fig. 4. RMS delay spread versus Tx–Rx distance at 38 GHz for LOS propagation, comparing antenna configurations C1 and C2.

4.2 Path loss (PL)

For propagation modeling, the CI model was employed, using path loss values measured at distances greater than 20 meters.

$$PL(D) = PL(d_0) + 10n \log_{10}\left(\frac{D}{d_0}\right) + X_\sigma \qquad (3)$$

where $PL(D)$is the path loss at distance D, $PL(d_0)$ is the free space path loss at the reference distance $d_0 = 1\ m$, n is the path loss exponent, is the shadow fading term, modeled as a zero mean Gaussian random variable with standard deviation σ

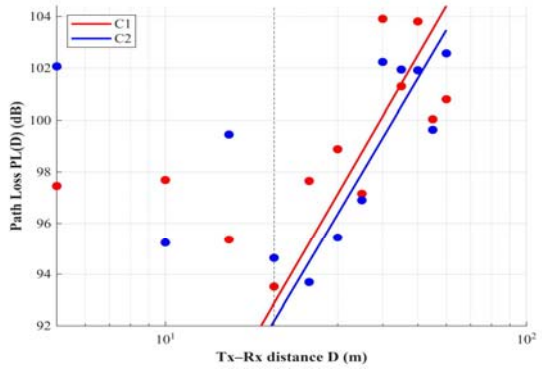


Fig. 5. Path loss as a function of Tx–Rx distance at 28 GHz for LOS propagation, for C1 and C2 antenna configurations.

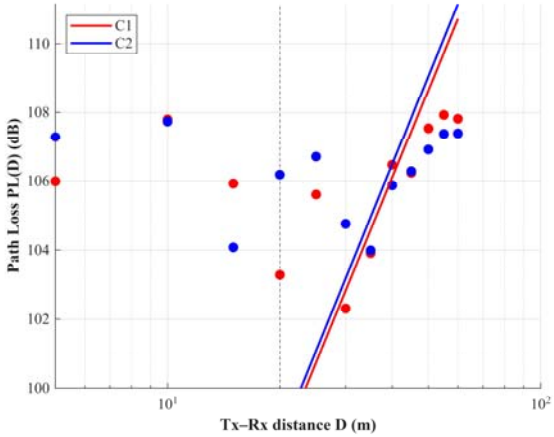


Fig. 6. Path loss as a function of Tx–Rx distance at 38 GHz for LOS propagation, for C1 and C2 antenna configurations.

Based on the measurements and the adapted CI model, the propagation loss exponent n was determined for 28 GHz and 38 GHz in two scenarios. At 28 GHz, n was similar in both scenarios (C1: 2.42; C2: 2.37), reflecting comparable propagation conditions and LOS dominance.

At 38 GHz, n slightly increased (C1: 2.63; C2: 2.65), indicating higher sensitivity to free-space losses at higher frequencies. Antenna geometry has minimal effect, while frequency has a greater impact on n, especially in the millimeter-wave range.

Table. 2. presents the shadow fading standard deviation obtained from the CI path loss model fitting for the analyzed measurement scenarios at 28 GHz and 38 GHz.

	C1	C2
Frequency	**dB**	**dB**
28 GHz	6.67	7.80
38 GHz	8.75	9.05

The shadow fading standard deviation indicates that antenna position affects signal stability. Lower values correlate with higher link stability, while higher values indicate increased fluctuations in received signal power.

5. Conclusion

An indoor corridor measurement campaign was conducted at 28 GHz and 38 GHz under LOS conditions, analyzing two scenarios: C1 – both antennas placed in the center, and C2 – the transmitter in the corner and the receiver in the center. Measurements were performed every 5 m along a 60 m corridor. Both path-loss and time-domain parameters, including RMS delay spread, were evaluated. The C2 configuration affects the temporal dispersion characteristics, influencing signal time consistency and link stability, although the RMS delay spread can be higher at short and medium distances. Path loss was modeled using the CI model; the propagation-loss exponent equals n = 2.4 at 28 GHz and n = 2.6 at 38 GHz, which is consistent with expectations. Antenna placement had a smaller impact than frequency. Analysis of the shadow fading standard deviation showed that the C2 configuration results in lower signal stability than C1 at both 28 GHz and 38 GHz, leading to increased signal-power fluctuations. The results confirm the significant influence of antenna position on signal stability and provide guidance for optimizing access-point placement in mmWave networks.

Acknowledgment

This work was supported in part by the National Science Centre, Poland, under the OPUS call in the Weave program under research project no. 2021/43/I/ST7/03294 acronym ‘MubaMilWave’, in part by the Military University of Technology under research project no. UGB 531-000128-W300-22/2026 on “Analysis of the possibility of using modern technologies in communication systems and electronic warfare”, and in part by the MeitY, Government of India, through the Chips-to-Startup program under project no. EE-9/2/2021-R&D-E.

References

[1] T. S. Rappaport, Y. Xing, G. R. MacCartney Jr., A. F. Molisch, E. Mellios, and J. Zhang,“Overview of millimeter wave communications for fifth-generation (5G) wireless networks—with a focus on propagation models,”IEEE Transactions on Antennas and Propagation, vol. 65, no. 12, Dec. 2017.

[2] O. Kanhere, H. Poddar, and T. S. Rappaport, “Calibration of NYURay for Ray Tracing Using 28, 73, and 142 GHz Channel Measurements Conducted in Indoor, Outdoor, and Factory Scenarios,” IEEE Trans. Antennas Propag., vol. 73, no. 1, pp. 405–420, Jan. 2025, doi: 10.1109/TAP.2024.3472214.

[3] 3GPP Tr 38.901 V17.0.0, 3rd Generation Partnership Project; „Technical Specification Group Radio Access Network; Study on channel model for frequencies from 0.5 to 100 GHz (Release 17),” march 2022.

[4] P. Zhang, J. Chen, X. Yang, N. Ma, and Z. Zhang, “Recent research on massive MIMO propagation channels: A survey,” IEEE Commun. Mag., vol. 56, no. 12, pp. 22–29, Dec. 2018, doi: 10.1109/MCOM.2018.1800196.

[5] Y. Wang, T. Wang, X. Zheng, X. Hao, and X. Liao, “Millimeter-wave and sub-THz radio propagation channel measurements and modeling in an indoor factory environment for ISAC,” IEEE Trans. Antennas Propag., vol. 73, no. 9, pp. 6883–6898, Sep. 2025

[6] N. Singh et al., “Channel modeling for 60 GHz fixed mmWave O2I and O2O uplink with angular misalignment,” IEEE Antennas Wirel. Propag. Lett., vol. 23, no. 5, pp. 1653–1657, May 2024.